RESEARCH ARTICLE

MXene-based Nanostructures for Water Splitting Process Using the Density Functional Theory

Sima Rastegar[1, 2, 3], Alireza Rastkar Ebrahimzadeh[1, 2, 3,*], Jaber Jahanbin Sardroodi[1, 2, 4]

[1] Molecular Simulation Laboratory (MSL), Azarbaijan Shahid Madani University, Tabriz, Iran

[2] Computational Nanomaterials Research Group (CNRG), Azarbaijan Shahid Madani University, Tabriz, Iran

[3] Department of Physics, Faculty of Basic Sciences, Azarbaijan Shahid Madani University, Tabriz, Iran

[4] Department of Chemistry, Faculty of Basic Sciences, Azarbaijan Shahid Madani University, Tabriz, Iran

ARTICLE INFO

Article History:
Received 2021-08-12
Accepted 2021-10-18
Published 2021-11-01

Keywords:
MXene
Photocatalyst
Water Splitting
DFT
Hybrid Functional

ABSTRACT

Solar energy reserving and conversion into usable chemical energy with semiconductor photocatalysts help a promising method to solve both energy and environmental issues. Green and efficient energy technologies are crucial where nanoscience could change the paradigm shift from fossil fuels to renewable sources. One of the most attractive cases is solar energy utilization to earn electricity or chemical fuel based on semiconductor nanomaterials' ability to function as photocatalysts promoting various oxidation and reduction reactions under sunlight. Recently, two-dimensional (2D) materials have attracted particular focus because of their charming properties. We report on a novel class of two-dimensional photocatalysts for hydrogen generation via water splitting. In this paper, by Density Functional Theory (DFT) calculations, we investigated Hf_2CO_2 as two-dimensional transition metal carbides, referred to as MXene, to understand its photocatalytic properties. Using this method, we theoretically investigated the structural, electronic, and optical properties of MXene-based nanostructures such as Hf_2CO_2 that calculated using GGA-PBE and HSE06 functionals. The lattice constant for GGA-PBE functional for Hf_2CO_2 is 3.3592A°. The calculated band gaps for GGA-PBE and HSE06 functionals for two-dimensional Hf_2CO_2 MXene were 0.92 and 1.75 eV, respectively. This MXene-based nanostructure also exhibits excellent optical absorption performance. Hence, Hf_2CO_2 is a promising photocatalytic material.

How to cite this article
*Rastegar S., Rastkar Ebrahimzadeh A., Jahanbin Sardroodi J. MXene-based Nanostructures for Water Splitting Process Using the Density Functional Theory. J. Nanoanalysis., 2021; 8(4): -10. DOI: 10.22034/jna.***.*

INTRODUCTION

The escalating consumption of fossil fuels has driven the development of energy generation methods to increase sustainability and reduce negative effects on the environment [1,2]. Nowadays, the much consumption of fossil fuels (natural gas, coal, oil, etc.) by population growth and continuous improvement of living standards have dramatically enhanced the world's demand for green energy. The large intake of fossil fuels has led to huge carbon dioxide (CO_2) emissions and global environmental challenges. Hence, various research effort are doing to find stable ways by using various strategies, such as solar energy, hydropower, wind energy, geothermal energy, and biomass energy [3–8]. Solar energy is considered one of the most promising options due to its ultimately unlimited supply. While natural photosynthesis is a biochemical process to transform sunlight, water, and carbon dioxide into carbohydrates and oxygen with very high efficiency, artificial photosynthesis is a human-made chemical process that biomimics the natural process of photosynthesis for catching and storing the energy from sunlight in the chemical bonds of solar fuels [9–14]. Photocatalytic water splitting and light-driven carbon dioxide reduction are two important applications. For the

* Corresponding Author Email: *a_rastkar@azaruniv.ac.ir*

past decades, various materials (organic, inorganic) have been designed for these purposes, such as graphene [15], TiO_2 [16], WO_3 [17], ABO_3 [18], Fe_2O_3 [19], WS_2 [20], MoS_2 [21], Bi_2O_3 [22] and $BiVO_4$ [23] etc. However, all these materials have some deficiencies, such as improper band gap or band edge positions, limited visible-light response, larger electronic defect density, and small surface area. Therefore, it is crucial to identify materials or a design strategy to overcome these deficiencies towards overall high efficiency for practical civil applications [24,25].

Photocatalytic water splitting can play an essential role in future renewable energy systems by presenting a way to directly convert solar energy into chemical energy in the form of hydrogen [26,27]. There are three steps in the process of water splitting using a semiconductor photocatalyst:

(1) Light absorption, resulting in electrons in the valence band is excited into the conduction band when a photon with energy major than the semiconductor's band gap energy is absorbed.

(2) Separation and diffusion of the photo-excited electrons and holes to the surface.

(3) The holes and electrons reduce surface reactions in which water, oxidized and protons, respectively, to produce O_2 and H_2 [28,29].

The photocatalytic water splitting process involves the generation of electrons and holes by photocatalysts through absorbing solar energy, the migration of the generated electrons and holes to the semiconductor surface, and the redox reaction of water to form H_2 and O_2 on the surface. In order to achieve these three steps, an ideal photocatalyst should meet the requirements of:

(1) A primary requirement for a suitable photocatalyst is that the conduction band minimum (CBM) should be higher (more negative) than the hydrogen reduction potential (H^+/H_2) and the valence band maximum (VBM) should be lower (more positive) than the water oxidation potential (H_2O/O_2) [30]. (2) Second, the smallest band gap for a semiconductor to be used as a photocatalyst is 1.23 eV.

Due to the wide range of applications of 2D nanomaterials in materials science, including energy storage [34], sensing [35], catalysis [36], and electronic devices [37] like field-effect transistors [38], caused to the 2D materials identify as a considerable research field. Recently, a new family of 2D materials has emerged known as MXenes. MXenes are a new family of 2D transition metal carbides/nitrides produced by selective chemical etching of "A" from MAX phases, where M is a transition metal, A is an IIIA or IVA element, and X is C or N [39]. Hydrogen produced by the direct splitting of water via a semiconductor photocatalyst under sunlight is considered an alternative energy resource to fossil fuels and a promising solution to severe environmental problems [40].

MXenes has highly regarded by researchers all over the world for its specific features. Currently, the potential of MXenes is due to their use as electrodes for supercapacitors [41], Li–S batteries [42], and Li-, Na- and K-ion batteries [43, 44]. All the MXenes are metals with a high electron density near the Fermi level [45]. Hence, all properties of MXenes could also be modified by surface functionalization [46-48]. Therefore, such materials convert from a metallic state to a semiconductor state due to surface functionalization by O or F groups. Also, the band gap can be tailored by surface functionalization [46, 47].

Band gap engineering is an essential technology for designing new materials and devices for semiconducting, optoelectronic, and optical applications [49, 50].

2D materials have two desirable advantages for water splitting: they have large surface active sites for photocatalytic reactions. The other is the thin layer allowing photogenerated electrons and holes to migrate rapidly, decreasing the possibility of electron-hole recombination and increasing the quantum yield [51-55].

In this paper, we study two-dimensional Hf_2CO_2 nanostructure from the family of MXenes. An important aim in our research is to study methods to discover photocatalyst for the water-splitting process. For this purpose, we calculate the structural, electronic, and optical properties of Hf_2CO_2 MXene, and using these properties, we find that it is a suitable and promising photocatalyst for the water-splitting process. For this work, we use the Vienna ab initio simulation package (VASP). Since the GGA-PBE always underestimates the band gap while a computationally more expensive Heyd–Scuseria– Ernzerhof (HSE06) hybrid functional [56] has been proven to provide accurate values agreeing well with experiments in a vast variety of systems.

COMPUTATIONAL METHOD

The computational studies based on Density Functional Theory (DFT) in conjunction with

projector augmented wave (PAW) potentials, as implemented in the Vienna ab initio simulation package (VASP) [57], which includes hybrid methods. Hybrid procedures generally increase the precision of computed band gaps compared with pure DFT computations [58]. The k-points of 11*11*1 and 13*13*1 were automatically generated by the Monkhorst–Pack scheme [59] used for structural optimization and static self-consistent calculations, respectively. The cutoff energy is set to be 520 eV. The optical absorption properties of the 2D semiconductor photocatalyst were studied using the calculation of dielectric constants (ε) at a given frequency. For this purpose, we used the Heyd-Scuseria-Ernzerhof (HSE06) hybrid functional with 11*11*1 k-point mesh. The atomic structures were analyzed by using the VESTA code.

RESULTS AND DISCUSSION

Among the two-dimensional MXene-based nanostructures with a hexagonal lattice, we can mention Hf_2CO_2. In this two-dimensional nanostructure, the C atom sandwiched between two layers of transition metal atoms functionalized with oxygen, shown in Fig. 1. The model shown in Fig. 1 is the most stable configuration after optimized geometry for the top (Fig. 1(a)) and side (Fig. 1(b)) views for two-dimensional MXene nanostructure, which is functionalized with oxygen.

To calculate the lattice parameter of Hf_2CO_2, corresponding simulated unit cells were optimized. Calculating the total energy of optimized primitive unit cells at different lattice parameters around the equilibrium lattice parameter and fitting the data with the Murnaghan equation of state [16], the

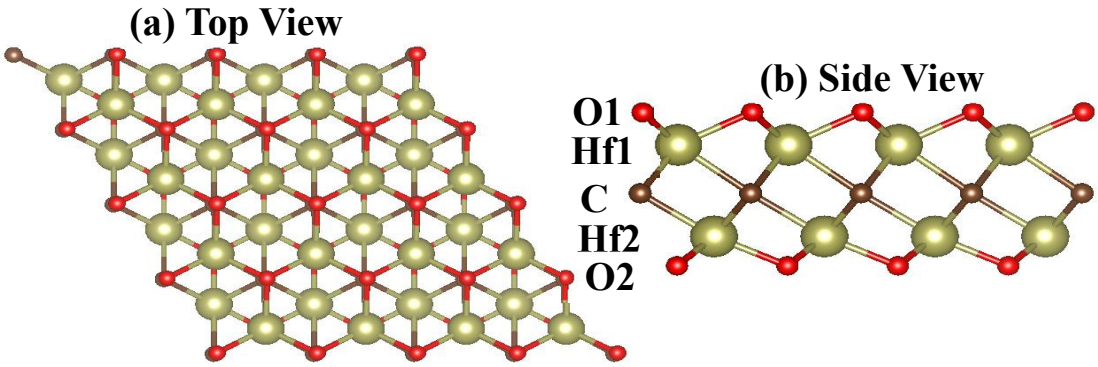

Fig. 1. (a) Top and (b) side views of the most stable configurations for two-dimensional Hf_2CO_2 MXene.

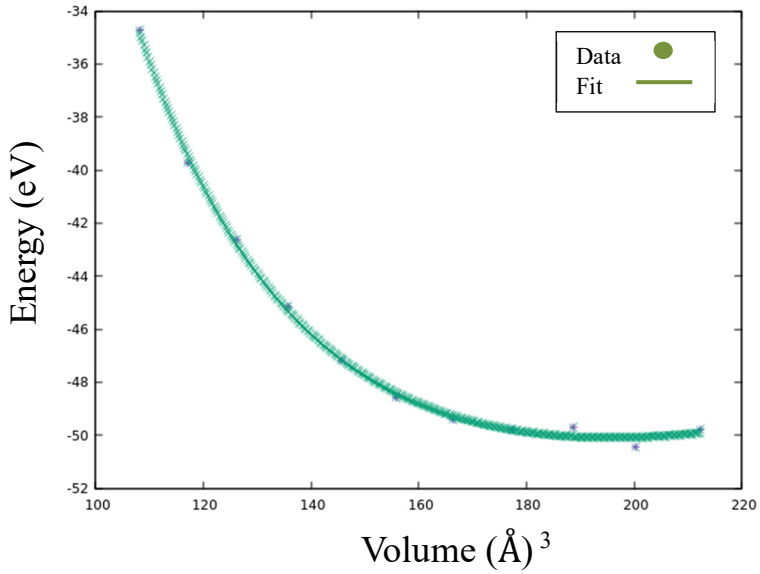

Fig. 2. Energy diagram based on unit cell volume for two-dimensional Hf_2CO_2 MXene and fitted curve.

obtained value of the equilibrium lattice parameter together with other theoretical result has been shown in Tabel 1. Fig. 2 shows the energy diagram based on unit cell volume for two-dimensional Hf_2CO_2 MXene and its fitted curve using the Birch-Murnaghan equation. This process was performed to obtain the best lattice constant for the structure two-dimensional Hf_2CO_2 MXene. The optimized lattice constant for Hf_2CO_2 using the GGA-PBE is 3.3592 A°, which is in excellent agreement with experimental and theoretical works [60]. The bond length for two-dimensional Hf_2CO_2 MXene is indicated in Table 2.

To explore the electronic properties of Hf_2CO_2, the electronic band structure that is pivotal in determining the electronic features has been determined for its structural geometry. The band structures of Hf_2CO_2 for GGA-PBE and HSE06 functionals were computed and are presented in Fig. 3. The computed band structures indicate that two-dimensional Hf_2CO_2 MXene, whether for GGA-PBE and HSE06, are semiconductors. In the present study and investigated reliable validations references for 2D Hf_2CO_2 MXene calculated bond length and energy gap indicated in Tables 2 and 3, respectively. The corresponding energy gap calculated with GGA-PBE and HSE06 functionals is 0.92 and 1.75 eV, respectively.

The density of states describes the distribution of electrons in the energy spectrum. One of the significant results obtained from their curvature is the compound's band gap. We have calculated the partial and total density of states using GGA-PBE and HSE06 approximations. The partial and total density of states for Hf_2CO_2 MXene with GGA-PBE and HSE06 functionals are presented in Fig. 4(a) and Fig. 4(b), respectively. The calculation of the partial density of states (PDOS) for M_2CT_2 materials is due to discovering the relationship between the band characteristics and the types and geometries of surface groups. As shown in Fig. 4, the p states from the C atom and the d states from the transition metal atom Hf are strongly hybridized, consistent with the fact that MXenes are assembled mainly through the bonds between C and transition metal atoms. The p states from the surface group O hybridize with the d states from the transition metal atom Hf, denoting strong covalent bonds between surface groups and transition metal atoms, which have theoretically verified to be responsible for the improvement of the mechanical flexibility of functionalized MXenes [48]. The most critical issue is that the two-dimensional Hf_2CO_2 MXene displays a more massive band gap than 1.23 eV, requiring the minimum value for photocatalytic water splitting. In chemistry, HOMO and LUMO are types of molecular orbitals. The HOMO and LUMO are the highest occupied molecular orbital and lowest unoccupied molecular orbital, respectively. Hence, we show HOMO and LUMO in Fig. 4(a) and 4(b).

In addition to the band gap size, we also computed the band edge positions for Hf_2CO_2 MXene. Band-edge positions are another predominant factor in facilitating the water-splitting reaction because the CBM and VBM must be higher (more negative) and lower (more positive) than the hydrogen reduction potential of H^+/H_2 and the water oxidation potential of H_2O/O_2, respectively. As shown in the schematic

Table 1. Lattice parameter for two-dimensional Hf_2CO_2 MXene.

Lattice parameter (Å)				
a (Present)	a (ref. 60)	a (ref. 61)	a (ref. 62)	a (ref. 63)
3.3592	3.2660	3.273	3.266	3.271

Table 2. Bond length for two-dimensional Hf_2CO_2 MXene.

Bond Length (Å)				
Hf1-Hf2	Hf1-C	Hf2-C	Hf1-O	Hf2-O
3.41	2.34	2.49	2.13	2.14

Table 3. Energy gap for two-dimensional Hf_2CO_2 MXene.

Energy gap (eV)			
E_g (GGA-PBE) (Present)	E_g (HSE06) (Present)	E_g (HSE06) (ref. 60)	Eg (HSE06) (ref. 62)
0.92	1.75	1.79	1.657

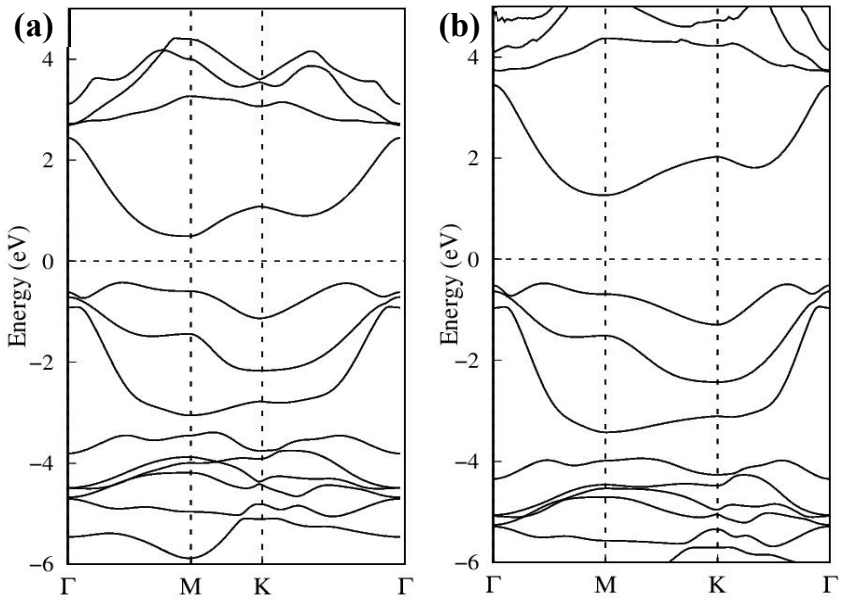

Fig. 3. Band structure for Hf_2CO_2 MXene for (a) GGA-PBE and (b) HSE06 functionals.

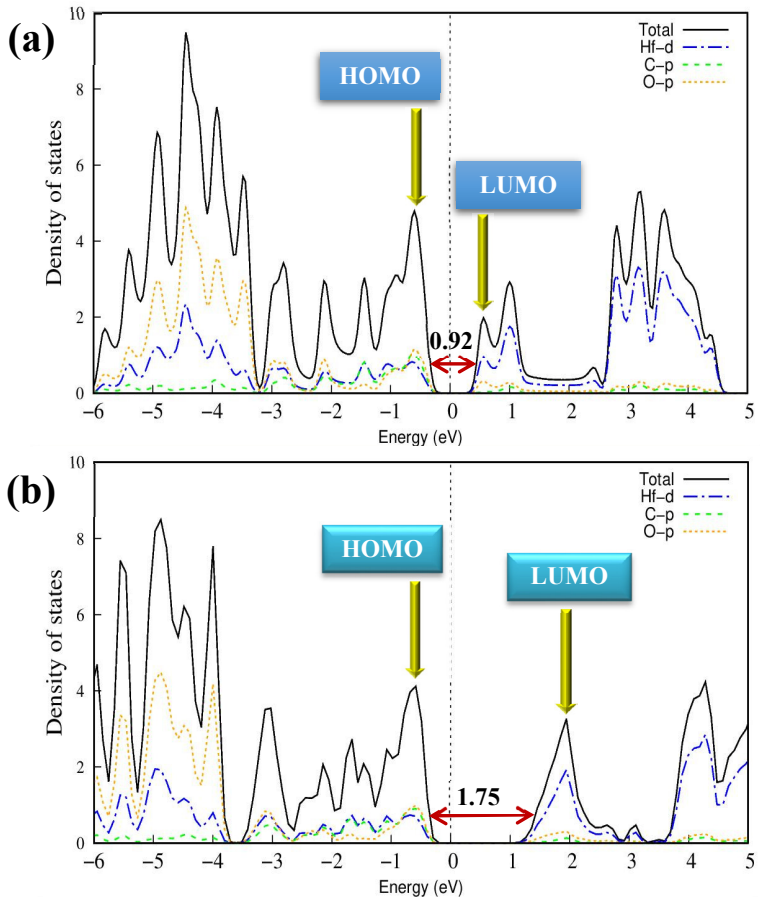

Fig. 4. The total density of states (TDOS) and projected density of states (PDOSs) of Hf_2CO_2 MXene for (a) GGA-PBE and (b) HSE06 functionals.

diagram (Fig. 5), the water oxidation and reduction processes for Hf_2CO_2 are thermodynamically feasible. Furthermore, this material's conduction band positions are high enough with respect to the water reduction potential, which means that the water reduction reaction's driving force is strong. Hence, two-dimensional Hf_2CO_2 material is a potential photocatalyst to drive the water-splitting reaction characterized by its appropriate band gap and band edge positions.

Optical properties play an essential role in determining and classifying materials that take advantage of solar cell systems. The study of optical properties is based on the calculation of absorption coefficients, which can be directly reached from the dielectric function. The optical spectrum provides a comprehensive source of information to study band structure, electronic properties, excitations, and network oscillations. Dielectric function is determined by the response of crystals to applied electromagnetic fields. One of the most critical optical quantities is the complex dielectric function, which describes the optical properties of a compound and is expressed by the following equation:

$$\varepsilon(\omega) = \varepsilon_1(\omega) + i\,\varepsilon_2(\omega) \quad (1)$$

Where $\varepsilon_1(\omega)$ and $\varepsilon_2(\omega)$ are the real and imaginary parts for dielectric function, respectively. The imaginary part of the dielectric function obtained from the following relation:

$$\varepsilon_2(\omega) = \frac{2e^2\pi}{\Omega\varepsilon_0}\sum\left|\left\langle\psi_K^C\left|\hat{u}.\vec{r}\right|\psi_K^V\right\rangle\right|\delta(E_K^C - E_K^V - E) \quad (2)$$

Where e is the electron charge, $\hat{u}$ is the unit vector of polarization the electric field, ψ_K^C and ψ_K^V are wave functions conduction and valence bands in K, respectively, and E_K^C E_K^V are related energies to these states.

The real contribution of the dielectric function is obtained by using the imaginary part as well as the Kramers-Kronig relation in the form of the following equation (2) [64].

$$\varepsilon_1(\omega) = 1 + \frac{2}{\pi}\mathrm{P}\int_0^\infty \frac{\omega'\varepsilon_2(\omega')}{\omega'^2 - \omega^2}d\omega' \quad (3)$$

The dielectric function has two intra-band and inter-band contributions. We do not consider indirect interband transitions that have a small contribution to the material's optical properties [65, 66]. We can obtain real contribution changes based on Kramers–Kronig transformations by having imaginary contribution changes [67].

The band structures of the Hf_2CO_2 indicate their visible-light absorption and possible photocatalytic applications. Therefore, we calculated the dielectric constants of the two-dimensional Hf_2CO_2 MXene using the HSE06 functional to confirm their optical

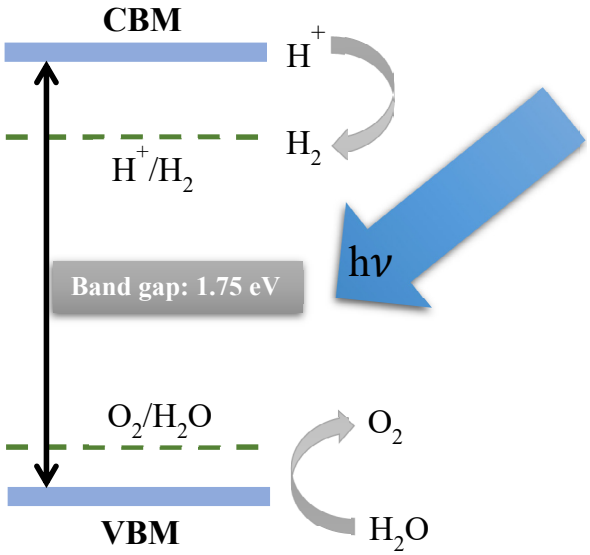

Fig. 5. Band edge positions and band gaps obtained by HSE06 functional for two-dimensional Hf_2CO_2 MXene.

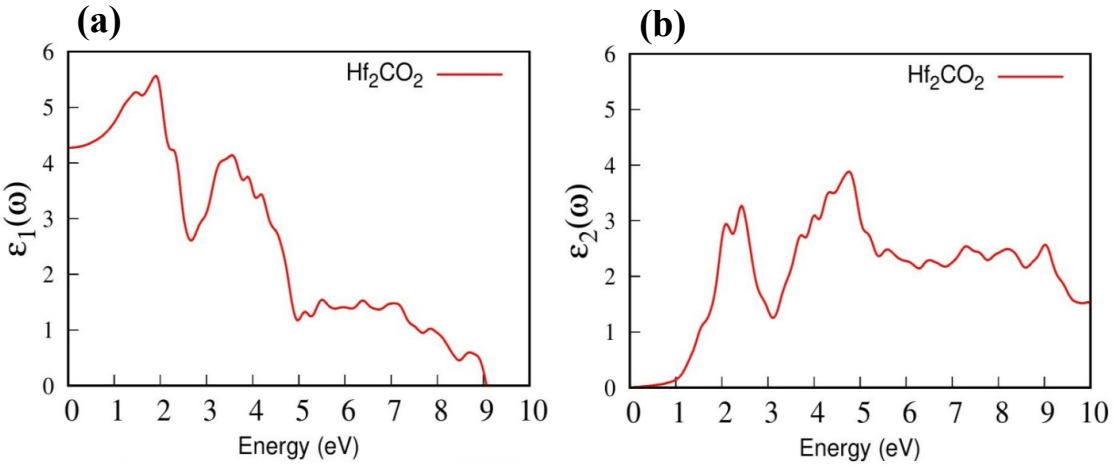

Fig. 6. Dielectric function for Hf_2CO_2, for (a) the real and (b) imaginary part.

absorption features. Dielectric function reality and imaginary parts are indicated in Fig. 6(a) and 6(b) for a two-dimensional Hf_2CO_2 structure.

From the dielectric function's real contribution, the static dielectric value is obtained, which is the dielectric function's value at zero energy. Fig. 6(a) illustrates the real contribution of the dielectric function for the 2D Hf_2CO_2 Mxene. According to Fig. 6(a), it can be seen that these structures show anisotropic behaviors in different directions.

As shown in Fig. 6(b), the imaginary part's positive value $\varepsilon_2(\omega)$ indicates the light absorption at a given frequency ω. The imaginary part $\varepsilon_2(\omega)$ results illustrate that 2D Hf2CO2 MXene functionalized by the –O group has visible light absorption due to the energies' positive values below 3.0 eV. The sizeable optical absorption of Hf_2CO_2 would guarantee high efficiency in the utilization of solar energy. Thus, this material has visible-light absorption and can probably be used as a visible-light-driven photocatalyst.

As shown in Fig. 6(b), the dielectric function's imaginary value up to 2eV is quiet that illustrated only intra-band transitions occur in this area. However, after this energy, this contribution suddenly increases, which indicates the absorption. Hence, after this sudden increase, inter-band transitions occur. Therefore, using the imaginary contribution, the dielectric function can be recognized optical gap of the material.

In the previous sections, in order to understand the photocatalytic behavior of Hf_2CO_2 for the process of water splitting, we calculated some of the inherent features like the structural, electronic, and optical properties. Consequently, to validate the present study's obtained results, we will use the previous theoretical and experimental analysis [60,62,68].

In a study aimed at investigating the photocatalytic properties of Hf_2CO_2 by ab initio calculations, they examined 48 two-dimensional (2D) transition metal carbides, also referred to as MXenes, to understand their photocatalytic stuff. Among the studied two-dimensional structures was Hf_2CO_2. They used the density functional theory method for all calculations. The optimized lattice constant for Hf_2CO_2 using the GGA-PBE was calculated at 3.2660 Å. The corresponding energy gap calculated HSE06 hybrid functional obtained 1.79 eV. Also, they showed that Hf_2CO_2 MXene exhibits excellent optical absorption performance in the wavelength ranging approximately 300 to 500 nm. Consequently, their calculations indicated that 2D Hf_2CO_2 is the just opportunity for photocatalysts for possible high-efficiency photocatalytic water splitting [60].

In other work, the thermal and electrical properties of oxygen-functionalized M_2CO_2 (M = Ti, Zr, Hf) MXenes are investigated using first-principles calculations. Their results show that Hf_2CO_2 is determined to be a semiconductor with a band gap of 1.657 eV and to have high and anisotropic carrier mobility [62].

Generally, it can be evaluated the efficacy of research studies by using theoretical and experimental investigation. The validity of its results is proved based on compliance with the relevant reference. Based on this point of view, we have

reviewed and evaluated the present study results by conforming to reliable experimental studies. Using these reliable scientific references to validate research results is a prevalent and formal way to achieve this goal. For the first time, in experimental research work, the application of two-dimensional (2D) layered transition metal carbides, MXenes, as electrocatalysts for the HER. Their computational screening study of 2D layered M_2XT_x (M = metal; X = (C, N); and T_x = surface functional groups) predicts Mo_2CT_x to be an active catalyst candidate for the HER. They also understand trends in HER activity among MXenes. Their study also contains the density functional theory (DFT) calculations to determine ΔG_H, a descriptor of HER activity, to a first approximation [68].

We have reviewed many such studies in detail on the structure of Hf_2CO_2 with different goals [61,63,69], but to validate our results, the mentioned cases seem enough.

As we mentioned in the sections on computed quantities, the values obtained for the lattice constant after optimization are 3.3592 Å, which we reached by applying the density functional theory method. According to Fig. 3(a) and 3(b), the measured amount of band gap for the 2D Hf_2CO_2 MXene using the GGA-PBE functional and HSE06 hybrid functional is 0.92 and 1.97 eV, respectively. In addition to the band gap size, we computed the band edge positions for 2D Hf_2CO_2 MXene. Also, as shown in Fig. 6(a) and 6(b), this structure has excellent optical absorption. Therefore, according to these interpretations, it can be said that this structure is a suitable photocatalyst for the water-splitting process. According to the research studies, to validate our work results, the agreement of the calculated results and the interpretations attributed to the studied structure with the validation reference to evaluate the accuracy and precision of the obtained quantities can be seen.

CONCLUSION

MXene-based materials have many attractive properties such as high surface area, tunable electronic structure, and high electronic conductivity. The mentioned features are proper for electrocatalysis applications. In order to further explore their application, it is needful to understand the MXene materials better. The present study systematically investigated the structural, electronic band structure, and optical properties of novel two-dimensional Hf_2CO_2 MXene using DFT calculations.

In this paper, to thoroughly explore the properties of MXenes as a photocatalyst for water splitting, we investigated the structural and electronic properties of Hf_2CO_2 MXene. The results indicate surface-functionalized M_2C-type MXenes, such as Hf_2CO_2, turn out to be semiconductors from GGA-PBE functional. Due to underestimate the band gaps in the calculations with the GGA-PBE functional, we computed the electronic structures using an HSE06 hybrid density functional. As shown in Fig. 3(b) and 4(b), a necessary condition for the water-splitting process was that the band gap for a suitable photocatalyst is 1.23 eV. Because this requirement could not be met by a GGA-PBE functional, we did this using an HSE06 hybrid functional, which caused the band gap to increase from 0.92 to 1.75 eV. Also, we illustrate the alignment of water reduction and oxidation potential for the band edges of MXenes to investigate the thermodynamic possibility of the water oxidation and reduction. Hence it seems that for Hf_2CO_2 MXene, the water oxidation and reduction processes are thermodynamically feasible. Furthermore, the optical absorption properties of two-dimensional Hf_2CO_2 are analyzed based on the dielectric function's calculated imaginary part. It can seem that this two-dimensional MXene-based nanostructure has a very high optical absorption and is suitable as a photocatalyst for the water-splitting process.

CONFLICT OF INTEREST

The authors declare that there is no conflict of interest regarding the publication of this manuscript.

REFERENCES

[1] Chu S, Majumdar A. Opportunities and challenges for a sustainable energy future. Nature. 2012;488(7411):294-303.
[2] Liang J, Chen D, Yao X, Zhang K, Qu F, Qin L, Huang Y, Li J. Recent Progress and Development in Inorganic Halide Perovskite Quantum Dots for Photoelectrochemical Applications. Small. 2020;16(15):1903398.
[3] Zheng S, Wang J, Sun C, Zhang X, Kahn ME. Air pollution lowers Chinese urbanites' expressed happiness on social media. Nature Human Behaviour. 2019;3(3):237-43.
[4] Singh R, Liu W, Lim J, Robel I, Klimov VI. Hot-electron dynamics in quantum dots manipulated by spin-exchange Auger interactions. Nature nanotechnology. 2019;14(11):1035-41.
[5] Qiao L, Xiao HY, Meyer HM, Sun JN, Rouleau CM, Puretzky AA, Geohegan DB, Ivanov IN, Yoon M, Weber WJ, Biegalski MD. Nature of the band gap and origin of the electro-/photo activity of Co_3O_4. Journal of Materials Chemistry C. 2013;1(31):4628-33.

[6] Huang YB, Liang J, Wang XS, Cao R. Multifunctional metal–organic framework catalysts: synergistic catalysis and tandem reactions. Chemical Society Reviews. 2017;46(1):126-57.
[7] Cai C, Han S, Liu W, Sun K, Qiao L, Li S, Zu X. Tuning catalytic performance by controlling reconstruction process in operando condition. Applied Catalysis B: Environmental. 2020;260:118103.
[8] Raziq F, Humayun M, Ali A, Wang T, Khan A, Fu Q, Luo W, Zeng H, Zheng Z, Khan B, Shen H. Synthesis of S-Doped porous g-C3N4 by using ionic liquids and subsequently coupled with Au-TiO2 for exceptional cocatalyst-free visible-light catalytic activities. Applied Catalysis B: Environmental. 2018;237:1082-90.
[9] Liu T, Liu D, Qu F, Wang D, Zhang L, Ge R, Hao S, Ma Y, Du G, Asiri AM, Chen L. Enhanced electrocatalysis for energy-efficient hydrogen production over CoP catalyst with nonelectroactive Zn as a promoter. Advanced Energy Materials. 2017;7(15):1700020.
[10] Feng JX, Xu H, Dong YT, Lu XF, Tong YX, Li GR. Efficient hydrogen evolution electrocatalysis using cobalt nanotubes decorated with titanium dioxide nanodots. Angewandte Chemie International Edition. 2017;56(11):2960-4. [11] Liu C, Colón BC, Ziesack M, Silver PA, Nocera DG. Water splitting–biosynthetic system with CO2 reduction efficiencies exceeding photosynthesis. Science. 2016;352(6290):1210-3.
[12] Wu X, He J, Zhang M, Liu Z, Zhang S, Zhao Y, Li T, Zhang F, Peng Z, Cheng N, Zhang J. Binary Pd/amorphous-SrRuO3 hybrid film for high stability and fast activity recovery ethanol oxidation electrocatalysis. Nano Energy. 2020;67:104247.
[13] Zhao Y, Zhao M, Ding X, Liu Z, Tian H, Shen H, Zu X, Li S, Qiao L. One-step colloid fabrication of nickel phosphides nanoplate/nickel foam hybrid electrode for high-performance asymmetric supercapacitors. Chemical Engineering Journal. 2019;373:1132-43.
[14] Gan J, He J, Hoye RL, Mavlonov A, Raziq F, MacManus-Driscoll JL, Wu X, Li S, Zu X, Zhan Y, Zhang X. α-CsPbI3 Colloidal Quantum Dots: Synthesis, Photodynamics, and Photovoltaic Applications. ACS Energy Letters. 2019;4(6):1308-20.
[15] Georgakilas V, Tiwari JN, Kemp KC, Perman JA, Bourlinos AB, Kim KS, Zboril R. Noncovalent functionalization of graphene and graphene oxide for energy materials, biosensing, catalytic, and biomedical applications. Chemical reviews. 2016;116(9):5464-519. [16] Lee BH, Park S, Kim M, Sinha AK, Lee SC, Jung E, Chang WJ, Lee KS, Kim JH, Cho SP, Kim H. Reversible and cooperative photoactivation of single-atom Cu/TiO 2 photocatalysts. Nature materials. 2019;18(6):620-6.
[17] Zheng G, Wang J, Liu H, Murugadoss V, Zu G, Che H, Lai C, Li H, Ding T, Gao Q, Guo Z. Tungsten oxide nanostructures and nanocomposites for photoelectrochemical water splitting. Nanoscale. 2019;11(41):18968-94.
[18] Tang M, Gao G, Rueda CB, Yu H, Thibodeaux DN, Awano T, Engelstad KM, Sanchez-Quintero MJ, Yang H, Li F, Li H. Brain microvasculature defects and Glut1 deficiency syndrome averted by early repletion of the glucose transporter-1 protein. Nature communications. 2017;8(1):1-5.
[19] Helal A, Harraz FA, Ismail AA, Sami TM, Ibrahim IA. Hydrothermal synthesis of novel heterostructured Fe2O3/Bi2S3 nanorods with enhanced photocatalytic activity under visible light. Applied Catalysis B: Environmental. 2017;213:18-27.
[20] Voiry D, Yamaguchi H, Li J, Silva R, Alves DC, Fujita T, Chen M, Asefa T, Shenoy VB, Eda G, Chhowalla M. Enhanced catalytic activity in strained chemically exfoliated WS 2 nanosheets for hydrogen evolution. Nature materials. 2013;12(9):850-5.
[21] Khan B, Raziq F, Faheem MB, Farooq MU, Hussain S, Ali F, Ullah A, Mavlonov A, Zhao Y, Liu Z, Tian H. Electronic and nanostructure engineering of bifunctional MoS2 towards exceptional visible-light photocatalytic CO2 reduction and pollutant degradation. Journal of hazardous materials. 2020;381:120972. [22] Hakobyan K, Gegenhuber T, McErlean CS, Müllner M. Visible-Light-Driven MADIX Polymerisation via a Reusable, Low-Cost, and Non-Toxic Bismuth Oxide Photocatalyst. Angewandte Chemie International Edition. 2019;58(6):1828-32. [23] Kuang Y, Jia Q, Ma G, Hisatomi T, Minegishi T, Nishiyama H, Nakabayashi M, Shibata N, Yamada T, Kudo A, Domen K. Ultrastable low-bias water splitting photoanodes via photocorrosion inhibition and in situ catalyst regeneration. Nature Energy. 2016;2(1):1-9.
[24] Liu CM, Lei MY, Yu H, Huang XY. Microstructure and photoluminescence of MoOx decorated ZnO nanorods. Chinese journal of physics. 2017;55(2):268-74.
[25] Wang Y, Yang H, Sun X, Zhang H, Xian T. Preparation and photocatalytic application of ternary n-BaTiO3/Ag/p-AgBr heterostructured photocatalysts for dye degradation. Materials Research Bulletin. 2020;124:110754.
[26] Zou Z, Ye J, Sayama K, Arakawa H. Direct splitting of water under visible light irradiation with an oxide semiconductor photocatalyst. nature. 2001;414(6864):625-7.
[27] Hisatomi T, Kubota J, Domen K. Recent advances in semiconductors for photocatalytic and photoelectrochemical water splitting. Chemical Society Reviews. 2014;43(22):7520-35.
[28] Maeda K. Photocatalytic water splitting using semiconductor particles: history and recent developments. Journal of Photochemistry and Photobiology C: Photochemistry Reviews. 2011;12(4):237-68.
[29] Maeda K, Domen K. New non-oxide photocatalysts designed for overall water splitting under visible light. The Journal of Physical Chemistry C. 2007;111(22):7851-61.
[30] Singh AK, Mathew K, Zhuang HL, Hennig RG. Computational screening of 2D materials for photocatalysis. The journal of physical chemistry letters. 2015;6(6):1087-98.
[31] Amin B, Kaloni TP, Schwingenschlögl U. Strain engineering of WS 2, WSe 2, and WTe 2. Rsc Advances. 2014;4(65):34561-5.
[32] Amin B, Singh N, Schwingenschlögl U. Heterostructures of transition metal dichalcogenides. Physical Review B. 2015;92(7):075439.
[33] Amin B, Kaloni TP, Schreckenbach G, Freund MS. Materials properties of out-of-plane heterostructures of MoS_2-WSe_2 and WS_2-$MoSe_2$. applied physics letters. 2016;108(6):063105.
[34] Zhao Y, Zhang Y, Yang Z, Yan Y, Sun K. Synthesis of MoS_2 and MoO_2 for their applications in H2 generation and lithium ion batteries: a review. Science and technology of advanced materials. 2013;14(4):043501.
[35] Late DJ, Huang YK, Liu B, Acharya J, Shirodkar SN,

Luo J, Yan A, Charles D, Waghmare UV, Dravid VP, Rao CN. Sensing behavior of atomically thin-layered MoS2 transistors. ACS nano. 2013;7(6):4879-91.

[36] Li Y, Wang H, Xie L, Liang Y, Hong G, Dai H. MoS2 nanoparticles grown on graphene: an advanced catalyst for the hydrogen evolution reaction. Journal of the American Chemical Society. 2011;133(19):7296-9.

[37] Xu K, Wang Z, Du X, Safdar M, Jiang C, He J. Atomic-layer triangular WSe2 sheets: synthesis and layer-dependent photoluminescence property. Nanotechnology. 2013;24(46):465705.

[38] Chhowalla M, Shin HS, Eda G, Li LJ, Loh KP, Zhang H. The chemistry of two-dimensional layered transition metal dichalcogenide nanosheets. Nature chemistry. 2013 Apr;5(4):263-75.

[39] Barsoum MW, Radovic M. Elastic and mechanical properties of the MAX phases. Annual review of materials research. 2011;41:195-227.

[40] Chen X, Liu L, Peter YY, Mao SS. Increasing solar absorption for photocatalysis with black hydrogenated titanium dioxide nanocrystals. Science. 2011;331(6018):746-50.

[41] Ghidiu M, Lukatskaya MR, Zhao MQ, Gogotsi Y, Barsoum MW. Conductive two-dimensional titanium carbide 'clay'with high volumetric capacitance. Nature. 2014;516(7529):78-81.

[42] Liang X, Garsuch A, Nazar LF. Sulfur cathodes based on conductive MXene nanosheets for high-performance lithium–sulfur batteries. Angewandte Chemie. 2015;127(13):3979-83.

[43] Mashtalir O, Naguib M, Mochalin VN, Dall'Agnese Y, Heon M, Barsoum MW, Gogotsi Y. Intercalation and delamination of layered carbides and carbonitrides. Nature communications. 2013;4(1):1-7.

[44] Xie Y, Dall'Agnese Y, Naguib M, Gogotsi Y, Barsoum MW, Zhuang HL, Kent PR. Prediction and characterization of MXene nanosheet anodes for non-lithium-ion batteries. ACS nano. 2014;8(9):9606-15.

[45] Naguib M, Kurtoglu M, Presser V, Lu J, Niu J, Heon M, Hultman L, Gogotsi Y, Barsoum MW. Two-dimensional nanocrystals produced by exfoliation of Ti3AlC2. Advanced materials. 2011;23(37):4248-53.

[46] Si C, Zhou J, Sun Z. Half-metallic ferromagnetism and surface functionalization-induced metal–insulator transition in graphene-like two-dimensional Cr2C crystals. ACS applied materials & interfaces. 2015;7(31):17510-5.

[47] Khazaei M, Arai M, Sasaki T, Chung CY, Venkataramanan NS, Estili M, Sakka Y, Kawazoe Y. Novel electronic and magnetic properties of two-dimensional transition metal carbides and nitrides. Advanced Functional Materials. 2013;23(17):2185-92.

[48] Guo Z, Zhou J, Si C, Sun Z. Flexible two-dimensional Ti n+ 1 C n (n= 1, 2 and 3) and their functionalized MXenes predicted by density functional theories. Physical Chemistry Chemical Physics. 2015;17(23):15348-54.

[49] Wu XK, Huang WQ, Huang ZM, Tang YL. Indirect to direct gap transition in low dimensional nanostructures of Silicon and Germanium. Physica E: Low-dimensional Systems and Nanostructures. 2017;90:24-7.

[50] Lin L, Li Z, Feng J, Zhang Z. Indirect to direct band gap transition in ultra-thin silicon films. Physical Chemistry Chemical Physics. 2013;15(16):6063-7.

[51] Hu W, Lin L, Zhang R, Yang C, Yang J. Highly efficient photocatalytic water splitting over edge-modified phosphorene nanoribbons. Journal of the American Chemical Society. 2017;139(43):15429-36.

[52] Lv X, Wei W, Sun Q, Li F, Huang B, Dai Y. Two-dimensional germanium monochalcogenides for photocatalytic water splitting with high carrier mobility. Applied Catalysis B: Environmental. 2017;217:275-84.

[53] Zhang X, Zhang Z, Wu D, Zhang X, Zhao X, Zhou Z. Computational screening of 2D materials and rational design of heterojunctions for water splitting photocatalysts. Small Methods. 2018;2(5):1700359.

[54] Wei Y, Ma Y, Wei W, Li M, Huang B, Dai Y. Promising Photocatalysts for Water Splitting in BeN2 and MgN2 Monolayers. The Journal of Physical Chemistry C. 2018;122(15):8102-8.

[55] Xiang Q, Yu J, Jaroniec M. Graphene-based semiconductor photocatalysts. Chemical Society Reviews. 2012;41(2):782-96.

[56] Marsman M, Paier J, Stroppa A, Kresse G. Hybrid functionals applied to extended systems. Journal of Physics: Condensed Matter. 2008;20(6):064201.

[57] Hafner J. Ab-initio simulations of materials using VASP: Density-functional theory and beyond. Journal of computational chemistry. 2008;29(13):2044-78.

[58] Muscat J, Wander A, Harrison NM. On the prediction of band gaps from hybrid functional theory. Chemical Physics Letters. 2001;342(3-4):397-401.

[59] Monkhorst HJ, Pack JD. Special points for Brillouin-zone integrations. Physical review B. 1976;13(12):5188.

[60] Guo Z, Zhou J, Zhu L, Sun Z. MXene: a promising photocatalyst for water splitting. Journal of Materials Chemistry A. 2016;4(29):11446-52.

[61] Khazaei M, Arai M, Sasaki T, Chung CY, Venkataramanan NS, Estili M, Sakka Y, Kawazoe Y. Novel electronic and magnetic properties of two-dimensional transition metal carbides and nitrides. Advanced Functional Materials. 2013;23(17):2185-92.

[62] Zha XH, Huang Q, He J, He H, Zhai J, Francisco JS, Du S. The thermal and electrical properties of the promising semiconductor MXene Hf2CO2. Scientific reports. 2016;6:27971.

[63] Fu CF, Li X, Luo Q, Yang J. Two-dimensional multilayer M_2CO_2 (M= Sc, Zr, Hf) as photocatalysts for hydrogen production from water splitting: a first principles study. Journal of Materials Chemistry A, 2017;5(47):24972-24980.

[64] Ambrosch-Draxl C, Sofo JO. Linear optical properties of solids within the full-potential linearized augmented planewave method. Computer physics communications. 2006;175(1):1-4.

[65] Landau LD, Lifshitz EM. Electrodynamics of continuous media Pergamon Press. Moscow, Russia. 1984. [66] Landau LD, Bell JS, Kearsley MJ, Pitaevskii LP, Lifshitz EM, Sykes JB. Electrodynamics of continuous media. elsevier; 2013. [67] Kramers HA. Brownian motion in a field of force and the diffusion model of chemical reactions. Physica. 1940;7(4):284-304.

[68] Seh ZW, Fredrickson KD, Anasori B, Kibsgaard J, Strickler AL, Lukatskaya MR, ... Vojvodic A. Two-dimensional molybdenum carbide (MXene) as an efficient electrocatalyst for hydrogen evolution. ACS Energy Letters, 2016;1(3):589-594.

[69] Gao G, O'Mullane AP, Du A. 2D MXenes: a new family of promising catalysts for the hydrogen evolution reaction. ACS Catalysis, 2017;7(1):494-500.